Supplementary Information

Title: Perturbation increases source-dependent organic matter degradation rates in estuarine sediments

Author information

Guangnan Wu[1], Klaas G.J. Nierop[2], Bingjie Yang[3], Stefan Schouten[3], Gert-Jan Reichart[1, 2], Peter Kraal[1]

[1] Royal Netherlands Institute for Sea Research, Department of Ocean Systems, Landsdiep 4, 1797 SZ ‘t Horntje, The Netherlands

[2] Utrecht University, Faculty of Geosciences, Princetonlaan 8a, 3584 CB Utrecht, The Netherlands

[3] Royal Netherlands Institute for Sea Research, Department of Marine Microbiology & Biogeochemistry, Landsdiep 4, 1797 SZ ‘t Horntje, The Netherlands

Corresponding author

Guangnan Wu (guangnan.wu@nioz.nl)

TABLE OF CONTENTS Page

Table. S1. Composition of artificial rainwater used in aerobic incubation experiments for moisture adjustment. The composition was based on the Dutch rainwater (Harpenslager et al., 2015). Chemicals were analytical grade dissolved in milli-Q water.

Salt	Concentration (mg/L)
NaCl	3.13
$MgSO_4 \cdot 7H_2O$	1.91
$MgCl_2 \cdot 6H_2O$	1.22
$CaCl_2 \cdot H_2O$	2.58
KCl	1.61

Table S2. MixSIAR modelled marine, riverine, and terrestrial contributions to the OM in 49 PoR sediments, respectively. Mean value and standard deviation are provided.

Sediment site	Marine contribution	Riverine contribution	Terrestrial contribution
201	45% ± 19.6%	32.7% ± 19.8%	22.3% ± 19.1%
130	49.9% ± 19.7%	28% ± 18%	22% ± 18.9%
93	27.5% ± 16.5%	36.3% ± 22%	36.2% ± 23.3%
131	58.1% ± 19.4%	23.7% ± 16.3%	18.2% ± 17.3%
202	41.5% ± 19%	21.7% ± 16.1%	36.8% ± 22.3%
117	49% ± 20.1%	32.4% ± 19.6%	18.7% ± 17.8%
90	50.5% ± 20%	28.3% ± 18.3%	21.3% ± 18.6%
89	58.4% ± 19.7%	24.8% ± 16.6%	16.9% ± 17.1%
94	55.5% ± 19.7%	25.8% ± 16.9%	18.7% ± 17.5%
123v1	42.6% ± 19.7%	36% ± 20.7%	21.4% ± 18.7%
115	57.4% ± 19.7%	26.3% ± 17.3%	16.3% ± 16.2%
140	63.4% ± 18.9%	19.8% ± 14.2%	16.8% ± 16.5%
114	62.2% ± 19.2%	22% ± 15.5%	15.8% ± 16.6%
204	32.6% ± 17.7%	34.6% ± 21%	32.8% ± 22.5%
86	63.6% ± 18.7%	20.3% ± 14.6%	16.1% ± 16%
C1	62.7% ± 19.2%	21.4% ± 15.2%	15.9% ± 16.3%
NWWG-09	22.9% ± 16.1%	48.4% ± 24.6%	28.8% ± 22.6%
73	37.3% ± 20.1%	42% ± 22.4%	20.7% ± 19.1%
76	33.8% ± 18.7%	41.1% ± 22.2%	25% ± 20.6%
80C	33.8% ± 18.9%	42.5% ± 22.7%	23.6% ± 20%
71	36.3% ± 19.4%	41.5% ± 22.4%	22.2% ± 19.8%
68	35% ± 19.3%	42.4% ± 22.6%	22.5% ± 20%
66	32.8% ± 18.6%	43.3% ± 22.9%	23.9% ± 20.1%
510	29.1% ± 18.3%	47.3% ± 23.7%	23.6% ± 20.6%
D1	22.5% ± 15.9%	48.2% ± 24.6%	29.3% ± 22.6%
56	32.5% ± 19%	45.6% ± 23.3%	22% ± 19.8%
51	34.6% ± 19.1%	41.2% ± 22.5%	24.2% ± 20.3%
31	31% ± 18.6%	46.3% ± 23.7%	22.7% ± 19.9%
50	26.4% ± 16.3%	37% ± 22.3%	36.7% ± 23.4%
34	27.6% ± 17.7%	47.4% ± 23.9%	25.1% ± 21%
K17	16.9% ± 12.9%	42.8% ± 24.4%	40.3% ± 24.8%
37	17% ± 13.7%	48.9% ± 25.4%	34.1% ± 24.2%
36	22% ± 15.7%	49.2% ± 24.7%	28.8% ± 22.7%
23	18.2% ± 15.4%	59.4% ± 25.4%	22.4% ± 20.9%
21A	24.7% ± 17%	51.2% ± 24.2%	24.1% ± 20.6%
S1	22.5% ± 16.1%	48.5% ± 24.5%	29% ± 22.6%
21Lv2	18.1% ± 15%	56.9% ± 25.4%	24.9% ± 21.5%
17	19.4% ± 14.6%	47.7% ± 24.8%	32.9% ± 23.7%
16	13.2% ± 10.5%	30.6% ± 21.5%	56.2% ± 24.2%
33	13.5% ± 10.8%	33.3% ± 22.5%	53.3% ± 24.6%

B16	13.8% ± 12.7%	55.4% ± 26.3%	30.8% ± 24.2%
B22	14.6% ± 13.2%	55.6% ± 25.8%	29.7% ± 23.6%
NWWG-02	55.9% ± 19.8%	27.3% ± 17.8%	16.8% ± 17.1%
NWWG-16	27.8% ± 17.2%	40.3% ± 22.9%	31.9% ± 22.8%
H4	21% ± 15.6%	48.6% ± 24.8%	30.5% ± 23.2%
84	10.8% ± 9.2%	30.3% ± 21.6%	58.9% ± 23.7%
NMS-18	23.3% ± 15.3%	38.2% ± 22.8%	38.4% ± 24%
14A	17.3% ± 13%	43.6% ± 24.5%	39.1% ± 24.6%
K1v2	24.8% ± 15.8%	12.4% ± 11.5%	62.8% ± 21.1%

Table. S3. Identified pyrolysis products, retention time, and their two fragment ions used to quantify and their assignment according to (Nierop et al., 2017). Types: Alk = *n*-alkenes/alkanes, Ar = aromatics or alkylbenzenes, Gua = guaiacols, Nt = N-containing compounds, Ph = phenols, Phy = phytadienes, Pri = pris-1-ene, Ps = polysaccharide-derived products, Syr = syringols. RT = retention time

RT	Pyrolysis product	*m/z*	Correction factor	Type
9.47	$C_{11:1}$	55+57	4.90	Alk
9.70	$C_{11:0}$	55+57	2.90	Alk
11.50	$C_{12:1}$	55+57	4.90	Alk
11.76	$C_{12:0}$	55+57	2.90	Alk
13.50	$C_{13:1}$	55+57	4.90	Alk
13.72	$C_{13:0}$	55+57	2.90	Alk
15.45	$C_{14:1}$	55+57	4.90	Alk
15.57	$C_{14:0}$	55+57	2.90	Alk
17.15	$C_{15:1}$	55+57	4.90	Alk
17.32	$C_{15:0}$	55+57	2.90	Alk
18.82	$C_{16:1}$	55+57	4.90	Alk
18.98	$C_{16:0}$	55+57	2.90	Alk
20.40	$C_{17:1}$	55+57	4.90	Alk
20.55	$C_{17:0}$	55+57	2.90	Alk
21.90	$C_{18:1}$	55+57	4.90	Alk
22.05	$C_{18:0}$	55+57	2.90	Alk
23.30	$C_{19:1}$	55+57	4.90	Alk
23.48	$C_{19:0}$	55+57	2.90	Alk
24.70	$C_{20:1}$	55+57	4.90	Alk
24.82	$C_{20:0}$	55+57	2.90	Alk
26.00	$C_{21:1}$	55+57	4.90	Alk
26.12	$C_{21:0}$	55+57	2.90	Alk
27.26	$C_{22:1}$	55+57	4.90	Alk
27.36	$C_{22:0}$	55+57	2.90	Alk
28.45	$C_{23:1}$	55+57	4.90	Alk
28.55	$C_{23:0}$	55+57	2.90	Alk
29.59	$C_{24:1}$	55+57	4.90	Alk
29.69	$C_{24:0}$	55+57	2.90	Alk
30.69	$C_{25:1}$	55+57	4.90	Alk
30.79	$C_{25:0}$	55+57	2.90	Alk
31.75	$C_{26:1}$	55+57	4.90	Alk
31.85	$C_{26:0}$	55+57	2.90	Alk
32.76	$C_{27:1}$	55+57	4.90	Alk
32.86	$C_{27:0}$	55+57	2.90	Alk
33.74	$C_{28:1}$	55+57	4.90	Alk
33.84	$C_{28:0}$	55+57	2.90	Alk
34.69	$C_{29:1}$	55+57	4.90	Alk

34.79	$C_{29:0}$	55+57	2.90	Alk
35.60	$C_{30:1}$	55+57	4.90	Alk
35.71	$C_{30:0}$	55+57	2.90	Alk
36.51	$C_{31:1}$	55+57	4.90	Alk
36.60	$C_{31:0}$	55+57	2.90	Alk
1.84	Benzene	78	1.90	Ar
2.97	Toluene	91+92	1.37	Ar
4.50	Ethylbenzene	91+106	1.60	Ar
4.68	1,3- and 1,4-Dimethylbenzene	91+106	1.60	Ar
5.01	Styrene	103+104	2.06	Ar
5.10	1,2-Dimethylbenzene	91+106	1.60	Ar
9.02	Guaiacol	109+124	1.92	Gua
11.21	4-Methylguaiacol	123+138	2.37	Gua
12.92	4-Ethylguaiacol	137+152	1.24	Gua
13.57	4-Vinylguaiacol	135+150	2.37	Gua
14.39	Eugenol	149+164	4.19	Gua
15.33	*cis*-Isoeugenol	149+164	4.19	Gua
16.06	*trans*-Isoeugenol	149+164	4.19	Gua
16.58	4-Acetylguaiacol	151+166	4.12	Gua
2.53	Pyridine	52+79	1.97	Nt
2.69	Pyrrole	67	1.67	Nt
3.98	2-Methylpyrrole	80+81	1.54	Nt
4.19	3-Methylpyrrole	80+81	1.54	Nt
4.36	4-Methylpyridine	66+93	1.93	Nt
9.67	Benzyl nitrile	90+117	2.38	Nt
11.68	Methylbenzylnitril	91+131	2.24	Nt
13.11	Indole	90+117	2.05	Nt
14.85	Methylindole	130+131	2.73	Nt
20.05	Diketodipyrrole	93+186	3.21	Nt
21.64	Diketopiperazine	70+154	5.20	Nt
23.20	Diketopiperazine	70+194	5.20	Nt
23.22	Diketopiperazine	70+154	5.20	Nt
7.17	Phenol	66+94	1.72	Ph
8.62	2-Methylphenol	107+108	2.93	Ph
9.10	3/4-Methylphenol	107+108	2.35	Ph
10.95	4-Ethylphenol	107+122	1.76	Ph
12.04	4-Vinylphenol	91+120	1.78	Ph
12.13	Catechol	64+110	2.42	Ph
22.58	Neophytadiene	68+82	5.79	Phy
22.91	*cis*-1,3-Phytadiene	68+82	6.80	Phy
23.19	*trans*-1,3-Phytadiene	68+82	6.80	Phy
21.02	Prist-1-ene	56+57	3.44	Pri
3.75	2-Furaldehyde	95+96	1.60	Ps

6.20	5-Methyl-2-furaldehyde	109+110	1.80	Ps
6.93	4-Hydroxy-5,6-dihydro-(2H)-pyran-2-one	58+114	1.60	Ps
9.02	Levoglucosenone	96+98	4.59	Ps
17.81	Levoglucosan	60+73	2.10	Ps
14.14	Syringol	139+154	2.38	Syr
15.93	4-Methylsyringol	153+168	2.94	Syr
17.32	4-Ethylsyringol	167+182	1.28	Syr
17.94	4-Vinylsyringol	165+180	3.03	Syr
18.57	4-Allylsyringol	179+194	3.08	Syr
19.37	*cis*-4-Prop-2-enylsyringol	179+194	3.08	Syr
20.14	*trans*-4-Prop-2-enylsyringol	179+194	3.08	Syr
20.57	4-Acetylsyringol	181+196	3.90	Syr

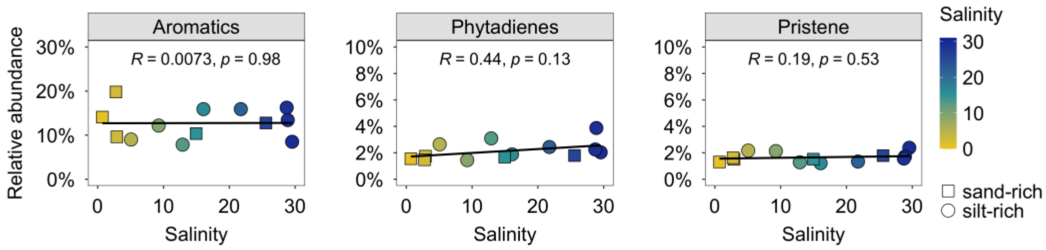

Fig. S1. Relative abundance of aromatics, phytadienes, and prist-1-ene in MOM pyrolysis products.

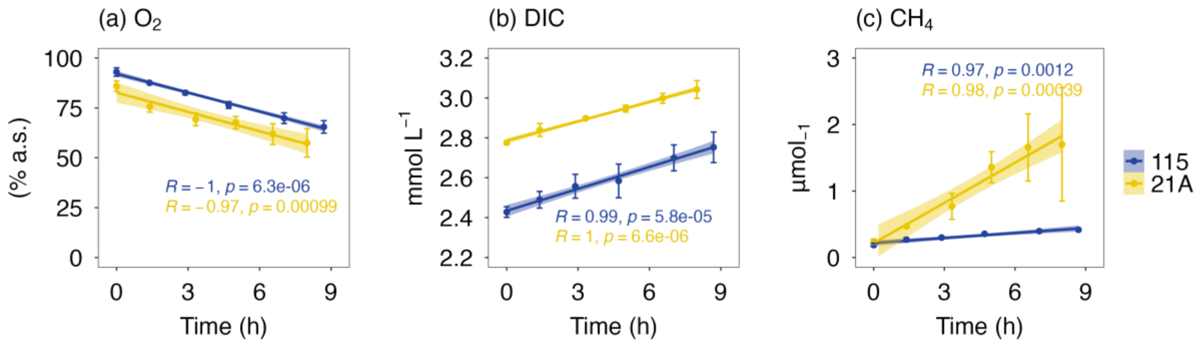

Fig. S2. The concentration of dissolved O_2, DIC, and CH_4 in the overlaying water over time during intact sediment core incubation.

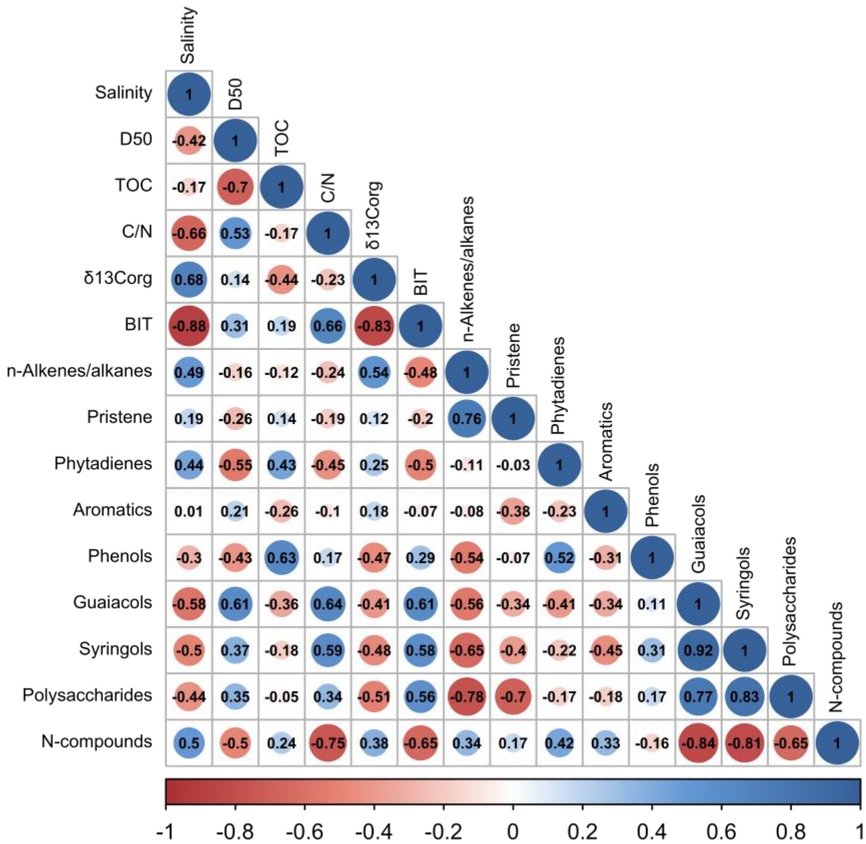

Fig. S3. The Pearson's correlation matrix of major sediment properties (i.e. salinity, D50, TOC) with sediment OM source proxies (i.e. CN, BIT index, and MOM pyrolysis products).

Theoretical diffusive fluxes of Fe^{2+}, S^{2-} and NH_4^+ and their contributions to the total measured benthic fluxes in the whole-core incubation experiment:

Diffusion fluxes of Fe^{2+}, S^{2-} and NH_4^+ were calculated from the measured Fe^{2+}, S^{2-} and NH_4^+ concentrations (Table S4) between the bottom water (5 cm above sediment-water interface) and porewater in top surface sediment slice (0–0.5 cm, average 0.25 cm below sediment-water interface) using Fick's first law:

$$J = -D\frac{dC}{dz}$$

where *J* is the diffusive flux (mol/(m^2 year)), *D* is the diffusion coefficient (m^2/year), *dC/dz* is the concentration gradient at the sediment-water interface (mol/m^4). The diffusion coefficients of Fe^{2+}, S^{2-} and NH_4^+ were obtain from the RStudio package '*marelac*' (Soetaert et al., 2023), considering the salinity (5.1 for 21A and 28.7 for 115) and temperature (22.7 ℃ for 21A and 18.7 ℃ for 115), further corrected for tortuosity (90% for both 115 and 21A) effect.

u

$$D_{corrected} = \frac{D}{1 - 2 \times \log{(porosity)}}$$

Table. S4 Major reducing species in the bottom water and porewater for sediment 115 and 21A.

	115		21A	
Species	Bottom water	Porewater	Bottom water	Porewater
Fe^{2+} (μM)	0.8	195.2	7.8	101.5
S^{2-} (mM)	0	1.91	0	1.57
NH_4^+ (μM)	421	1109	186	798

The calculated diffusive fluxes of Fe^{2+}, S^{2-} and NH_4^+ were 0.098 mmol m^{-2} d^{-1}, 0.0049 mmol m^{-2} d^{-1} and 0.0018 mmol m^{-2} d^{-1} for sediment 115 and 8.5×10^{-5} mmol m^{-2} d^{-1}, 0.0046 mmol m^{-2} d^{-1} and 0.0018 mmol m^{-2} d^{-1} for sediment 21A. Assuming all diffusive Fe^{2+}, S^{2-} and NH_4^+ were all oxidized by O_2, the oxidation of Fe^{2+}, S^{2-} and NH_4^+ consumed 0.038 mmol O_2 m^{-2} d^{-1} for sediment 115 and 0.013 mmol O_2 m^{-2} d^{-1} for 21A, which contributed to less than 0.12% of the total O_2 consumption rates for both 21A and 115.

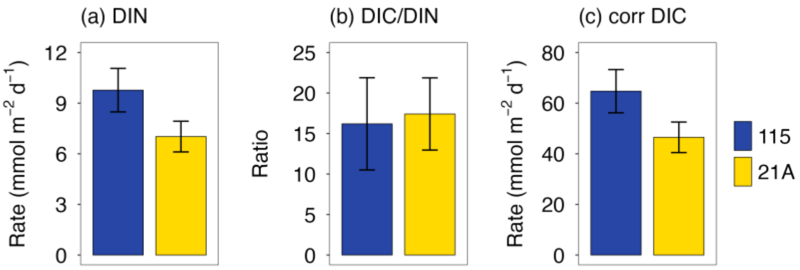

Fig. S4. (a) Benthic fluxes of dissolved inorganic nitrogen (DIN); (b) ratio of DIC flux to DIN flux; (c) DIN-corrected DIC.

Assuming OM degradation generated DIC and DIN following Redfield ratio (C:N = 106:16), we calculate DIN-corrected DIC (Fig. S4c), which accounts for ~40% of the total DIC flux (Fig. 5b). This suggests around 40% of DIC was produced from OM degradation, among which 50–71% of DIC was generated aerobically when compared to O_2 consumption rates (Fig. 5a).

References

Harpenslager, S. F., Van Dijk, G., Kosten, S., Roelofs, J. G. M., Smolders, A. J. P., and Lamers, L. P. M.: Simultaneous high C fixation and high C emissions in Sphagnum mires, Biogeosciences, 12, 4739–4749, https://doi.org/10.5194/bg-12-4739-2015, 2015.

Nierop, K. G. J., Reichart, G. J., Veld, H., and Sinninghe Damsté, J. S.: The influence of oxygen exposure time on the composition of macromolecular organic matter as revealed by surface sediments on the Murray Ridge (Arabian Sea), Geochim Cosmochim Acta, 206, 40–56, https://doi.org/10.1016/j.gca.2017.02.032, 2017.

Soetaert, K., Petzoldt, T., Meysman, F., and Meire, L.: marelac: Tools for Aquatic Sciences, https://cran.r-project.org/web/packages/marelac/index.html, 2023.